한국기계가공학회지, 제20권, 제10호, pp. 19～26(2021.10) ISSN 1598-6721(Print)
Journal of the Korean Society of Manufacturing Process Engineers, Vol. 20, No. 10, pp. 19~26(2021.10) ISSN 2288-0771(Online)

https://doi.org/10.14775/ksmpe.2021.20.10.019

Surface-shape Processing Characteristics and Conditions during Trajectory-driven Fine-particle–injection Processing

Hyoung-Tae Lee*, Chul-Woong Hwang*, Sea-Han Lee**, and Duck Hyun Wang**,#
*Graduate School, Kyungnam Univ., **School of Mechanical Engineering, Kyungnam Univ.

궤적 구동 미세입자 분사가공 시 표면 형상 가공 특성 및 가공 조건

이형태*, 황철웅*, 이세한**, 왕덕현**,#
*경남대학교 대학원,**경남대학교 기계공학부

(Received 30 July 2021; received in revised form 06 August 2021; accepted 20 August 2021)

ABSTRACT

In fine-particle–injection processing, hard fine particles, such as silicon carbide or aluminum oxide, are injected using high-pressure air, and a small amount of material is removed by applying an impact to the workpiece by spraying at high speeds. In this study, a two-axis stage device capable of sequence control was developed to spray various shapes, such as circles and squares, on the surface during the micro-particle jetting process to understand the surface-shape micro-particle-processing characteristics. In the experimental device, two stepper motors were used for the linear movement of the two–degree-of-freedom mechanism. The signal output from the microcontroller is converted into a signal with a current sufficient to drive the stepper motor. The stepper motor rotates precisely in synchronization with the pulse-signal input from the outside, eliminating the need for a separate rotation-angle sensor. The major factors of the processing conditions are fine particles (silicon carbide, aluminum oxide), injection pressure, nozzle diameter, feed rate, and number of injection cycles. They were identified using the ANOVA technique on the design of the experimental method. Based on this, the surface roughness of the spraying surface, surface depth of the spraying surface, and radius of the corner of the spraying surface were measured, and depending on the characteristics, the required spraying conditions were studied.

Keywords : Micro Particle Blasting Machining(미세입자 분사가공), Particle(분사입자), Blasting Pressure(분사 압력), Experimental Analysis(실험분석), Analysis of Variance(분산분석)

1. Introduction

Microparticle blasting is a process of injecting hardened microparticles, such as silicon carbide or aluminum oxide, using high air pressure and blasting them at high speed to impact and remove a small quantity of the workpiece.

The technique to apply particle blasting to the manufacturing of microstructures is called microparticle blasting. In recent years, this technique has gained attention as a mechanical processing method for brittle materials that can be applied to the manufacturing of semiconductor parts,

Corresponding Author : dhwang@kyungnam.ac.kr
Tel: +82-55-249-2712, Fax: +82-505-999-2160

micromachine parts, and flat panels. Moreover, it is used in manufacturing to increase the surface roughness for improving the adhesiveness of the titanium alloy used for implants.[1-3]

This study aims to develop a two-axis stage equipment that can control the sequence and investigate the surface shape of microparticles for blasting various shapes such as circles and squares onto the surface during the microparticle blasting[5].

Two-step motors were used for the linear transfer with a two-degree-of-freedom mechanism motion. The signal coming out from the microcontroller was converted to the signal with the electric current in a size suitable for step motor operation. Furthermore, by revolving the step motor to be precisely synchronized with the pulse signal inputted from the outside, no separate rotational angle sensor was needed.

Using the analysis of variance (ANOVA) technique of the design of experiments methodology[4], the main factors of the processing conditions, namely microparticle (silicon carbide and aluminum oxide), blasting pressure, nozzle diameter, feed rate, and number of blast cycles were identified, the roughness of the blasting processed surface, blasting maximum depth, and blasted surface corner radius were measured, and the suitable blasting conditions were investigated based on these properties.

2. Experimental Equipment and Methods

Table 1 Specifications of micro drive device

Item	Specification
x-axis blasting range	100mm
y-axis blasting range	80mm
Resolution x-y axis (drive unit)	5㎛
blasting speed	0.5 ~ 10mm/sec (0.5unit)
blasting cycle	1.0 ~ 10cycle (1.0unit)
Square	Trajectory 1 ~30mm (1.0unit)

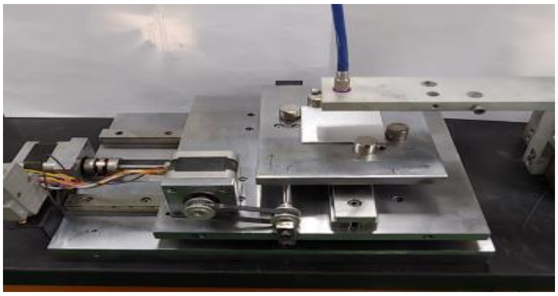

Fig. 1 Micro drive device with sequence control

The two-axis fine drive unit that can perform sequence control is the equipment used inside the Dual tank micro blaster (MB1006) for the microparticle blasting. The two-axis stage fine drive unit that can control the sequence was developed for the experiments of this study to prevent the effect of microparticle infiltration into the driving part on the operation due to the high-speed blasting and to ensure a smooth operation. This equipment that materializes the plane two-degree-of-freedom operation and is composed of a two-degree-of-freedom mechanism.

The stage moves in X-axis and Y-axis directions, and the orthogonal system mechanism is used for the prevention of interference of each axis. The highly reliable conversion into rotary-rectilinear movement was materialized using the ball-screw, and a precise position control without backlash using two-step motors was secured. Furthermore, the stability of the motion was secured using the contact of the limit sensor. Figure 1 presents the fine drive unit that can perform sequence control, and Table 1 presents the motion specifications of the drive unit.

All functions of the experimental equipment are controlled by the microcontroller ATMEGA 2560. When the electric power is input, ATMEGA 2560 stops the step motor, performs the initialization, which sets up the setting of the experimenter to the specific values, displays the standby status on the screen when the initialization is completed, and waits for the input of the experimenter at the

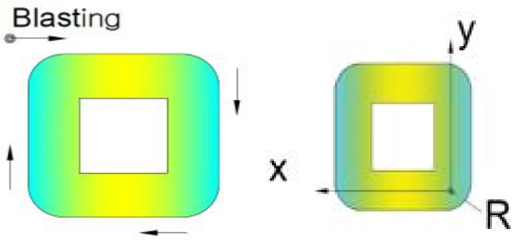

(a)Blasting process (b)Measurement section

Fig. 2 Square trajectory for fine particle blasting process

standby status.

In the case of the blasting process using the two-degree-of-freedom sequence controlled microparticle transfer equipment, the movement was controlled in a square trajectory with 16 mm on a side. During this process, to identify the conditions required for the testing and main factors required for processing, we investigated the main factors that have a significant impact on the experimental conditions and results.

Fig. 2 (a) shows the schematic diagram of the square trajectory controlled during the microparticle blasting, and Fig. 2 (b) shows the measurement range of the X-axis, Y-axis, and R after the blasting.

In this experiment, the microparticles were sprayed on the aluminum A1050-T2 specimen. In the preliminary tests, we hypothesized that among the blasting conditions of the blast equipment, such as microparticle sprayer, with higher pressure and larger nozzle diameter, the surface shape change would proportionally increase. To verify these hypotheses, the blasting tests were conducted by polarizing the values of the processing conditions such as particle type, pressure, nozzle diameter, feed rate, and number of blast cycles and setting up these conditions at two levels. Based on the results, we investigated the relationship between the surface roughness of the blast processed surface and surface blasting depth under different processing conditions through the measured data values.

For identifying the relationship between the experimental conditions of the preliminary tests and hypotheses and materializing the process, the blasting experiments were performed by reducing the processing range levels used in the preliminary tests and operating in the square trajectory with 16 mm on a side using the sequence controlled blasting equipment.

After conducting the experiments, the relationship between the main factors and results was analyzed using the ANOVA technique. The surface roughness and blast maximum depth in the X-axis direction were compared with those in the Y-axis direction during the microparticle blasting, and the main factors were identified under the blasting conditions, with reduced processing range levels. After the preliminary tests, five factors, namely (A) blasting particle, (B) nozzle diameter, (C) blasting pressure, (D) feed rate, and (E) number of blast cycles, were selected as the primary experimental factors. For the factors of the blasting of the surface shape, two-level comparison factors were generated, the generated factors were randomly arranged, and the data were produced via each test to identify more important factors. Each factor was set to have two levels (i.e., 0 and 1). The factors were composed of (A) blasting particle (0: SiC, 1: Al_2O_3), (B) nozzle diameter (0: Ø0.7mm, 1: Ø1.5mm), (C) blasting pressure (0: 200kPa, 1: 350kPa), (D) feed rate (0: 1mm/s, 1: 3mm/s), and (E) number of blast cycles (0: 1 cycle, 1: 3 cycles).

Based on these conditions, the experimental plan was set up using the table of orthogonal arrays, and five-factor columns out of seven columns were randomly selected and arranged as presented in Table 2. After naming the five factors as A, B, C, D, and E, and arranging them to the column numbers 1, 2, 3, 4, and 5, respectively, the experimental conditions of the factors were determined as follows. Because error (e) was used in the arrangement of column numbers 6 and 7, the degree of freedom of the error term became 2 during the ANOVA. In terms of the factor level, the levels 0 and 1 were arranged to the numberS 0 and 1 displayed in the table, respectively.

In these experiments, the prepared specimens were used based on the experimental order determined according to the design of experiments methodology. Silicon carbide (SiC) and aluminum oxide (Al_2O_3) with particle sizes of 50μm were used as microparticle abrasives, and the blasting was conducted at a blasting height of 25mm. For the three main factors determined in the primary tests, (A) blasting particle was set to have 2 levels, and (B) blasting nozzle diameter and (C) blasting pressure were set to have 4 levels. The experiments were conducted while keeping the other factors, (D) feed rate, (E) number of blast cycles, and (F) blasting height, at fixed values.

Table 2 In place of the five factors $L_8(2^7)$

No.	Experimental procedure	Column index							Experimental condition
		1	2	3	4	5	6	7	
1	3	0	0	0	0	0	0	0	$A_0B_0C_0D_0E_0$
2	2	0	0	0	1	1	1	1	$A_0B_0C_0D_1E_1$
3	4	0	1	1	0	0	1	1	$A_0B_1C_1D_0E_0$
4	1	0	1	1	1	1	0	0	$A_0B_1C_1D_1E_1$
5	5	1	0	1	0	1	0	1	$A_1B_0C_1D_0E_1$
6	8	1	0	1	1	0	1	0	$A_1B_0C_1D_1E_0$
7	7	1	1	0	0	1	1	0	$A_1B_1C_0D_0E_1$
8	6	1	1	0	1	0	0	1	$A_1B_1C_0D_1E_0$
Fundamental Presentation		a	b	a b	c	a c	b c	a b c	
Batch		A	B	C	D	E	e	e	

Table 3 Factor and levels for micro blasting experiment for aluminium A1050-T2

Symbol	Factors	Levels			
		1	2	3	4
A	Particle (50㎛)	SiC		Al_2O_3	
B	Nozzle diameter (mm)	∅0.46	∅0.7	∅1.16	∅1.5
C	Pressure (KPa)	200	350	500	650
D	Feedrate (mm/sec)	3			
E	Blast cycle number (cycle)	3			
F	Height blasting (mm)	25			

3. Results and Discussion

Using the ANOVA technique, the main factors of the processing conditions, namely the microparticles of SiC and Al_2O_3, nozzle diameter, blasting pressure, number of blast cycles, and feed rate, were identified.

By measuring the surface roughness of the two-axis blasted surface in the grain direction of the specimen, maximum depth of the blast processed surface, and corner radius of the blast processed surface, and analyzing these characteristics with the ANOVA technique, the conditions for the optimum surface shape processing during the trajectory driving microparticle blasting were identified and the following experimental results were obtained.

For the surface roughness, the centerline average roughness (Ra) and 10-point average roughness (Rz) values were measured in a micrometer (μm) unit using the Stylus surface roughness measuring instrument. In this study, the experimental data were tabulated based on Ra values.

As shown in Table 4, the P-value of the blasting particle, nozzle diameter, and blasting pressure were found to be 0.003, 0.002, and 0.000, respectively, based on the X-axis ANOVA results. For P-values below 0.05, the effect of the corresponding factor on the experiments was considered as significant. However, as is difficult to identify which factor has a more significant impact only based on the P-values.

Therefore, this aspect was evaluated based on the contribution of factors affecting the surface roughness Ra. The contributions of the blasting particle, nozzle diameter, and blasting pressure were found to be 27.18%, 15.88%, and 42.33%, respectively. Thus, the blasting pressure had a more significant effect, followed by blasting particle and nozzle diameter.

Figure 3 shows a plot of the factors with more significant effect on the surface roughness Ra in the

X-axis direction.

In terms of the factor level, level 1 of the blasting particle refers to SiC and level 2 to Al_2O_3. The levels 1, 2, 3, and 4 of the nozzle diameter are Ø0.46mm, Ø0.7mm, Ø1.16mm, and Ø1.5mm, respectively, and those of the blasting pressure are 200kPa, 350kPa, 500kPa, and 650kPa, respectively.

Based on the analysis results of the factors at each level, the effect of level 1 (SiC) was higher for the blasting particle. In the case of the nozzle diameter, the effect increased up to level 3 (Ø1.16mm) and decreased for level 4 (Ø1.5mm). Unlike the nozzle diameter, the effect of the blasting pressure increased with increasing the level.

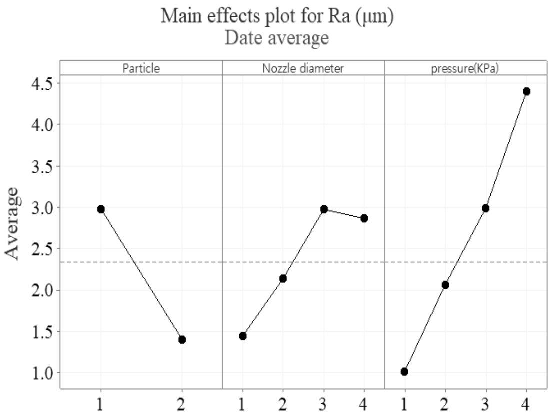

Fig. 3 Main effect diagram according of surface roughness Ra in x-axis direction

Table 4 ANOVA results of surface roughness Ra measurement in x-axis direction

Source	DF	Seq SS	level of contribution (%)	Adj SS	Adj MS	F	P
Particle	1	16.222	27.28%	5.348	5.3478	11.77	0.003
Nozzle diameter (mm)	3	9.444	15.88%	10.391	3.4637	7.63	0.002
Pressure (kPa)	3	25.172	42.33%	25.172	8.3907	18.47	0.000
Error	19	8.629	14.51%	8.629	0.4542		
Total	26	59.467	100.00%				

As presented in Table 5, based on the X-axis ANOVA results, the P-values of the blasting particle, nozzle diameter, and blasting pressure were found to be 0.013, 0.005, and 0.000, respectively (level of significance: P-value ≤ 0.05).

Furthermore, based on the contribution of factors affecting the blasted maximum depth, the contributions of blasting particle, nozzle diameter, and blasting pressure were 25.14%, 14.10%, and 44.50%, respectively. Thus, the blasting pressure had a more significant effect, followed by blasting particle and nozzle diameter.

Table 5 ANOVA results of surface max depth measurement in x-axis direction

Source	DF	Seq SS	level of contribution (%)	Adj SS	Adj MS	F	P
Particle	1	2476	25.14%	636.3	636.34	7.55	0.013
Nozzle diameter (mm)	3	1389	14.10%	1467.6	489.21	5.80	0.005
Pressure (kPa)	3	4384	44.50%	4383.6	1461.20	17.34	0.000
Error	19	1601	16.26%	1601.3	84.28		
Total	26	9850	100.00%				

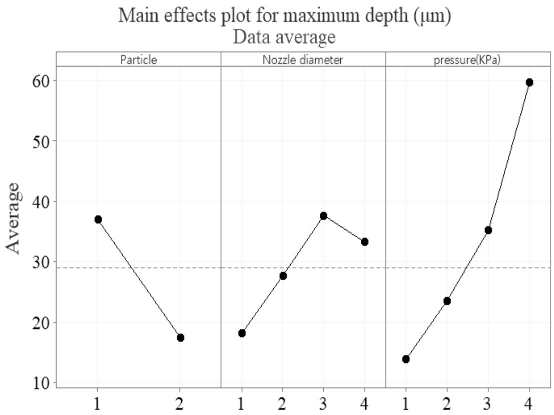

Fig. 4 Main effect diagram according of surface max depth in x-axis direction

Figure 4 shows a plot of the factors with more significant effects on the blasted surface maximum depth in the X-axis direction. Based on the analysis results of the factors at different levels, the effect of level 1 (SiC) was higher for the blasting particle. In terms of the nozzle diameter, the highest impact was observed at level 3 (Ø1.16mm) and decreased for level 4 (Ø1.5mm). Unlike the nozzle diameter, the effect of the blasting pressure rapidly increased at level 4 (650kPa).

Table 6 ANOVA results of surface roughness Ra measurement in y-axis direction

Source	DF	Seq SS	level of contribution (%)	Adj SS	Adj MS	F	P
Particle	1	17.046	28.08%	5.870	5.8698	12.71	0.002
Nozzle diameter (mm)	3	9.552	15.73%	10.478	3.4928	7.56	0.002
Pressure (kPa)	3	25.333	41.73%	25.333	8.4442	18.28	0.000
Error	19	8.777	14.46%	8.777	0.4620		
Total	26	60.707	100.00%				

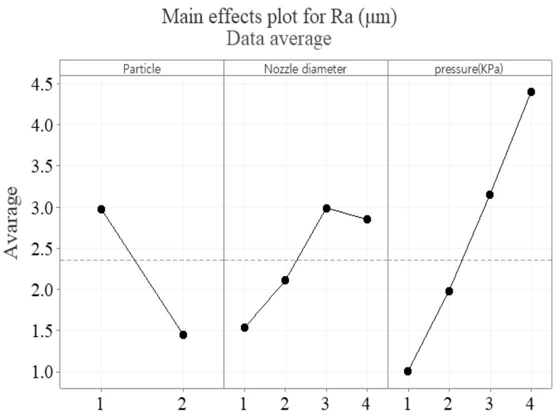

Fig. 5 Main effect diagram according of surface roughness Ra in y-axis direction

Table 6 shows the ANOVA results of the surface roughness Ra in the Y-axis direction. As presented, the P-values of the blasting particle, nozzle diameter, and blasting pressure were 0.002, 0.002, and 0.000, respectively (level of significance: P-value ≤ 0.05). The contributions of blasting particle, nozzle diameter, and blasting pressure were 28.08%, 15.73%, and 41.73%, respectively. Thus, the blasting pressure had a more significant effect, followed by blasting particle and nozzle diameter.

Figure 5 presents a plot of the factors with more significant effects on the center line average roughness Ra in the Y-axis direction. Based on the analysis results of the factors at different levels, the effect of level 1 (SiC) was higher than that of level 2 (Al_2O_3) for the blasting particle. In terms of the nozzle diameter, the highest impact was observed at level 3 (Ø1.16 mm) and decreased for level 4 (Ø1.5 mm). Unlike the nozzle diameter, the effect of the blasting pressure rapidly increased at a higher level.

As shown in Table 7, based on the ANOVA results of the blasted surface maximum depth in the X-axis direction, the P-values of the blasting particle, nozzle diameter, and blasting pressure were 0.028, 0.016, and 0.000, respectively, indicating that their effect on the blasted surface maximum depth was significant. Furthermore, the contributions of the blasting particle, nozzle diameter, and blasting pressure

Table 7 ANOVA results of surface max depth measurement in y-axis direction

Source	DF	Seq SS	level of contribution (%)	Adj SS	Adj MS	F	P
Particle	1	2428	24.44%	668.2	668.2	5.64	0.028
Nozzle diameter (mm)	3	1414	14.24%	1586.5	528.8	4.47	0.016
Pressure (kPa)	3	3841	38.67%	3841.0	1280.3	10.81	0.000
Error	19	2250	22.65%	2250.0	118.4		
Total	26	9934	100.00%				

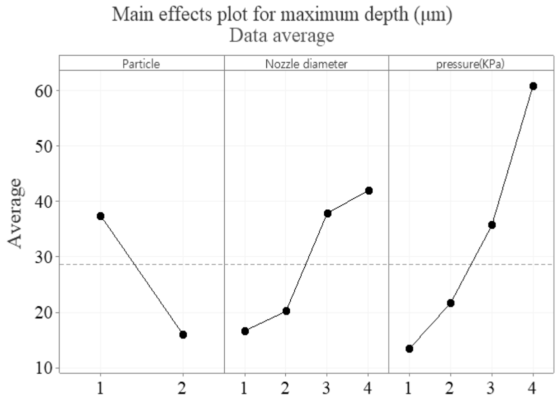

Fig. 6 Main effect diagram according of surface max depth in y-axis direction

were 24.44%, 14.24%, and 38.67%, respectively. Thus, the blasting pressure had a more significant effect, followed by blasting particle and nozzle diameter.

Figure 6 shows a plot of the factors with more significant effects on the blasted surface maximum depth in the Y-axis direction. Based on the analysis results of the factors at different levels, the effect of level 1 (SiC) was higher than that of level 2 (Al_2O_3) for the blasting particle. In terms of the nozzle diameter, highest impact was observed at levels 3 (Ø1.16 mm) and 4 (Ø1.5 mm). In addition, the effect of the blasting pressure rapidly increased at a higher level.

To identify the classification power of each blasting condition of the specimen through the main factors, the blasted surface corner radii of the specimens No. 1 to No. 16, processed with blasting particles SiC or Al_2O_3, were measured using the tool microscope, and the results are tabulated in Table 8. Based on the data of the specimens No. 1 to No. 16 processed with the blasting particle SiC, the corner radii were at nozzle diameter and blasting pressure of Ø0.46mm and 200kPa, Ø1.5mm and 350kPa, Ø1.5mm and 500kPa, and Ø1.5mm and 650kPa, respectively, were 5.008mm, 7.291mm, 9.690mm, and 11.509mm. For the specimens No. 1 to No. 16 processed with the blasting particles Al_2O_3, the shapes at the nozzle diameter of Ø0.46mm and Ø1.5mm appeared large.

Table 8 Measured corner radius values

No.	Argument SiC	Coner Radius (mm)	No.	Argument Al_2O_3	Coner Radius (mm)
1	A1 B1 C1 D1 E1	5.008	1	A2 B1 C1 D1 E1	3.503
2	A1 B2 C1 D1 E1	3.814	2	A2 B2 C1 D1 E1	2.039
3	A1 B3 C1 D1 E1	4.976	3	A2 B3 C1 D1 E1	2.452
4	A1 B4 C1 D1 E1	4.536	4	A2 B4 C1 D1 E1	2.372
5	A1 B1 C2 D1 E1	5.251	5	A2 B1 C2 D1 E1	3.420
6	A1 B2 C2 D1 E1	3.361	6	A2 B2 C2 D1 E1	2.148
7	A1 B3 C2 D1 E1	5.293	7	A2 B3 C2 D1 E1	2.683
8	A1 B4 C2 D1 E1	7.291	8	A2 B4 C2 D1 E1	2.658
9	A1 B1 C3 D1 E1	6.582	9	A2 B1 C3 D1 E1	4.204
10	A1 B2 C3 D1 E1	4.502	10	A2 B2 C3 D1 E1	1.720
11	A1 B3 C3 D1 E1	8.524	11	A2 B3 C3 D1 E1	3.107
12	A1 B4 C3 D1 E1	9.690	12	A2 B4 C3 D1 E1	2.710
13	A1 B1 C4 D1 E1	6.415	13	A2 B1 C4 D1 E1	4.042
14	A1 B2 C4 D1 E1	5.587	14	A2 B2 C4 D1 E1	2.512
15	A1 B3 C4 D1 E1	9.770	15	A2 B3 C4 D1 E1	3.207
16	A1 B4 C4 D1 E1	11.509	16	A2 B4 C4 D1 E1	4.518

4. Conclusions

In this study, the two-axis drive unit with the sequence control enabled, which can perform the microparticle blasting with various trajectories such as specific points, circles, and squares, was developed and the blasting was conducted under various experimental conditions. The following conclusions were drawn from the study.

1. In the surface microblasting processing experiments with the square drive trajectory, the effects of blasting pressure on the centerline average roughness (Ra) and blasted surface maximum depth were more significant, followed by the effects of blasting particle and nozzle diameter;
2. The contributions of the blasting pressure,

blasting particle, and blasting nozzle diameter on the surface roughness (Ra) in the X-axis direction were 44.50%, 25.14%, and 14.10%, respectively, and those on the surface roughness (Ra) in the Y-axis direction were 47.52%, 25.91%, and 14.75%, respectively, indicating that the X-axis and Y-axis directions follow the same tendency;

3. In terms of the blasting particle, the effect of SiC silicon carbide was more significant. For the blasting nozzle, the effect of level 3 (Ø1.16mm) was more significant than that of level 4 (Ø1.5mm), suggesting that up to the nozzle diameter of Ø1.16mm, the blasting force with the increase of pressure is maintained, but when the nozzle diameter increases to Ø1.5mm, the pressure is dispersed. For the blasting pressure, its impact was at the highest at level 4 (650kPa). In terms of the main effect on the blasted surface maximum depth in the Y-axis direction, the effect of SiC was more significant at levels 3 (Ø1.16mm) and 4 (Ø1.5mm) of the blasting nozzle diameter, and the impact of blasting pressure was the highest at level 4 (650kPa);
4. The corner radius of the blasted surface processed with SiC was large at the blasting pressure of level 4 (650kPa) with a minimum of 3.361mm and a maximum of 11.509mm, whereas the corner radius of the blasted surface processed with Al_2O_3 had a minimum of 1.720mm, a maximum of 4.518mm, and average of 2.559mm. Based on the analysis results of the average radius of each nozzle, the lowest average radius was obtained when the nozzle diameter was Ø0.7mm, indicating stable blasting. When using SiC, the corner radius was found to increase with increasing nozzle diameter.

REFERENCES

1. Kwon, D. G., Wang, D. H., "Optimal Blasting Conditions for Surface Profile when Micro Particle Blasting by Statistical Analysis of Orthogonal Arrays," Journal of the Korean Society of Manufacturing Process Engineers, Vol. 15, No. 4, pp. 148-154, 2016.
2. Hwang, C. W., Lee, S. H., Wang, D. H., “Selection of Main Factors by Experimental Analysis for Profile Blast Machining Based on Microparticle Blasting Equipment with a Two-Axis Sequence Control Stage”, Journal of the Korean Society of Manufacturing Process Engineers, Vol. 19, No. 11, pp. 64~69, 2020.
3. Hwang, C. W., Lee, S. H., Wang, D. H., “A Study on the Development of a 2-axis Stage with Sequence Control for Micro Particle Blast Machining”, Journal of the Korean Society of Manufacturing Process Engineers, Vol. 19, No. 8, pp. 81～87, 2020.
4. Kim, S. H., Wang, D. H., Lee, S. H., “The Characteristics of Surface Roughness when Micro Blasting of Titanium Alloy with Spiral Movement”, Journal of the Korean Society of Manufacturing Process Engineers, Vol. 11, No, 4, pp. 125-130, 2012.
5. Jang, H. S., Kim, H. S., Shin, K. H., "A Study on Performance Improvement of Electrical Discharge Machining for Producing Micro-holes Using a Shot Blasting Surface Treatment", Transactions of Materials Processing, Vol. 21 No. 5, pp. 312-318, 2012.